Title

The Use of Spatial and Spatiotemporal Modeling for Surveillance of H5N1 Highly Pathogenic Avian Influenza in Poultry in the Middle East

Journal

Avian Diseases, 60(1s)

ISSN

0005-2086

Authors

Alkhamis, Mohammad
Hijmans, Robert J
Al-Enezi, Abdullah
et al.

Publication Date

2016-05-01

DOI

10.1637/11106-042115-reg

Peer reviewed

The Use of Spatial and Spatiotemporal Modeling for Surveillance of H5N1 Highly Pathogenic Avian Influenza in Poultry in the Middle East

Author(s): Mohammad Alkhamis, Robert J. Hijmans, Abdullah Al-Enezi, Beatriz Martínez-López and Andres M. Perea

Source: Avian Diseases, 60(1s):146-155.
Published By: American Association of Avian Pathologists
https://doi.org/10.1637/11106-042115-Reg
URL: http://www.bioone.org/doi/full/10.1637/11106-042115-Reg

AVIAN DISEASES 60:146–155, 2016

Research Article—

The Use of Spatial and Spatiotemporal Modeling for Surveillance of H5N1 Highly Pathogenic Avian Influenza in Poultry in the Middle East

Mohammad Alkhamis,[ABE] Robert J. Hijmans,[C] Abdullah Al-Enezi,[A] Beatriz Martínez-López,[D] and Andres M. Perea[B]

[A]Environmental and Life Sciences Research Center, Kuwait Institute For Scientific Research, P.O. Box 24885, Safat 13109, Kuwait
[B]Veterinary Population Medicine Department, Veterinary Medical Center, University of Minnesota, St. Paul, MN 55108
[C]Department of Environmental Science and Policy, One Shields Avenue, University of California, Davis, CA 95616
[D]Center for Animal Disease Modeling and Surveillance, Department of Medicine and Epidemiology, School of Veterinary Medicine, One Shields Avenue, University of California, Davis, CA 95616

Received 23 April 2015; Accepted 6 January 2016; Published ahead of print 12 January 2016

SUMMARY. Since 2005, H5N1 highly pathogenic avian influenza virus (HPAIV) has severely impacted the economy and public health in the Middle East (ME) with Egypt as the most affected country. Understanding the high-risk areas and spatiotemporal distribution of the H5N1 HPAIV in poultry is prerequisite for establishing risk-based surveillance activities at a regional level in the ME. Here, we aimed to predict the geographic range of H5N1 HPAIV outbreaks in poultry in the ME using a set of environmental variables and to investigate the spatiotemporal clustering of outbreaks in the region. Data from the ME for the period 2005–14 were analyzed using maximum entropy ecological niche modeling and the permutation model of the scan statistics. The predicted range of high-risk areas ($P > 0.60$) for H5N1 HPAIV in poultry included parts of the ME northeastern countries, whereas the Egyptian Nile delta and valley were estimated to be the most suitable locations for occurrence of H5N1 HPAIV outbreaks. The most important environmental predictor that contributed to risk for H5N1 HPAIV was the precipitation of the warmest quarter (47.2%), followed by the type of global livestock production system (18.1%). Most significant spatiotemporal clusters ($P < 0.001$) were detected in Egypt, Turkey, Kuwait, Saudi Arabia, and Sudan. Results suggest that more information related to poultry holding demographics is needed to further improve prediction of risk for H5N1 HPAIV in the ME, whereas the methodology presented here may be useful in guiding the design of surveillance programs and in identifying areas in which underreporting may have occurred.

RESUMEN. Uso de los modelos espaciales y espacio-temporales para la vigilancia de la influenza aviar altamente patógena H5N1 en la avicultura del Medio Oriente.

Desde el año 2005, el virus de la influenza aviar altamente patógeno H5N1 (HPAIV) ha impactado severamente la economía y la salud pública en el Oriente Medio, siendo Egipto el país más afectado. La comprensión de las zonas de alto riesgo y la distribución espacio-temporal del virus de la influenza de alta patogenicidad H5N1 en aves comerciales es un requisito previo para el establecimiento de actividades de vigilancia basados en el riesgo a nivel regional en el Oriente Medio. En este estudio, se intentó predecir el alcance geográfico de los brotes del virus de la influenza de alta patogenicidad H5N1 en aves comerciales en el Oriente Medio utilizando un conjunto de variables ambientales, para investigar la agrupación espacio-temporal de los brotes en la región. Los datos provenientes del Oriente Medio para el período entre el año 2005 al 2014 se analizaron mediante modelos de máxima entropía de nichos ecológicos y por el modelo de permutación de las estadísticas de rastro. El rango previsto de zonas de alto riesgo ($P > 0.60$) para el virus de influenza aviar de alta patogenicidad H5N1 en la avicultura incluye partes de los países de la parte noreste del Oriente Medio, mientras que el delta del Nilo y el valle en Egipto se estimaron que eran los lugares más adecuados para la presentación de brotes de influenza aviar de alta patogenicidad H5N1. El predictor ambiental más importante que contribuyó al riesgo del virus H5N1 fue la precipitación del trimestre más cálido (47.2%), seguido por el tipo de sistema de producción ganadera global (18.1%). La mayoría de los grupos de espacio-temporales significativos ($P < 0.001$) fueron detectados en Egipto, Turquía, Kuwait, Arabia Saudita y Sudán. Los resultados sugieren que se necesita más información relacionada con la demografía de las zonas avícolas para mejorar aún más la predicción de riesgo para el virus de la influenza aviar de alta patogenicidad H5N1 en el Oriente Medio, mientras que la metodología que aquí se presenta puede ser útil para enfocar el diseño de programas de vigilancia y en la identificación de áreas en las que puede haber ocurrido subregistro.

Key words: H5N1, highly pathogenic avian influenza, Middle East, surveillance, maximum entropy, scan statistics

Abbreviations: AI = avian influenza; AUC = area under the curve; cAUC = calibrated AUC; FAO = Food and Agriculture Organization of the United Nation; HPAIV = highly pathogenic avian influenza virus; IBA = important bird areas; Maxent = presence-only maximum entropy ecological niche modeling; ME = Middle East; OIE = World Organization for Animal Health; RAMSAR = Convention on Wetlands of International Importance; ROC = receiver operator characteristic; SSB = spatial sorting bias

Emergence and reemergence of highly pathogenic avian influenza virus (HPAIV) is a concern for countries and governments because of its impact on the public health and economy. Growth of the domestic poultry sector in response to the rapid increase in global demand for protein, as well as climate change, increase of international trade, and land cover fragmentation, have been considered as important risk factors for the continuous global increase in the incidence of emerging zoonoses such as avian influenza (AI) viruses, including in Middle East (ME) countries (11,27,29,36,48).

[E]Corresponding author. E-mail: mkhamis@kisr.edu.kw

The first novel emergence of H5N1 HPAIV occurred in commercial domesticated geese in Guandong province in China in 1996 (60). Since then, the ancestral strain of H5N1 HPAIV has continued to circulate within Asia and consequently has undergone numerous genetic changes leading to the evolution of different lineages, sometimes also referred to as clades (38). Within the ME, Turkey was the first country to report H5N1 HPAIV, in backyard poultry, in October 2005. Subsequently, more than 1000 cases were reported in Egypt, Iraq, Iran, Israel, Jordan, Kuwait, Palestinian Territories, Sudan, and Djibouti between November 2005 and April 2006. In 2007, Saudi Arabia was the last country to report a series of H5N1 outbreaks, whereas Libya reported their first single introduction in 2014 (41). Countries in the region that have never reported the disease include Bahrain, Qatar, United Arab Emirates, Eritrea, Somalia, and Yemen. During the first Eurasian pandemic wave (2006–07), the H5N1 HPAIV caused substantial socioeconomic losses in the ME, with Egypt being the most affected country. As of October 2014, Egypt reported more than 2500 outbreaks in poultry, which, at the time, was the highest number of reported outbreaks outside South East Asia (17). Because of that high reported incidence, Egypt has been considered by some as the epicenter of the H5N1 HPAIV in the ME (1,28). Control measures in the region varied among countries but mostly included a stamping out policy, quarantine, movement restrictions, zoning, and vaccination (8). AI surveillance activities included active and passive strategies, with few countries making use of molecular techniques, whereas most made use of serologic tests for detection (8). In general, intensive AI surveillance activities in the ME countries are not routinely conducted, and, instead, are only triggered by the emergence of epidemic levels, such as those detected in 2005–07.

Because wild birds are natural reservoirs for AI viruses and are considered the main source for disease transmission into poultry, it has been hypothesized that early detection of AI in poultry would be maximized by early detection of infection in wild birds (51). Consequently, the European Union has established guidelines for the surveillance of AI in wild birds, intended to maximize the efficiency of surveillance efforts as an alternative to random sampling, by intensifying sampling in areas, species, and at times at which the probability of H5N1 HPAIV outbreaks was predicted to increase, and to aid in adjusting control and prevention resources accordingly (7,20). However, this action is justified because the number of H5N1 cases in wild birds was substantially higher than those detected in the ME during the 2005–07 pandemic. Indeed, the total number of H5N1 HPAIV detected cases in wild birds in the ME region did not exceed 1% from the reported incidences between 2005 and 2014 (18).

The dynamics of AI virus spread and geographic distribution are influenced by the environmental conditions of the setting (33,39,44,55). Ecologic niche modeling offers the possibility to build predictive distribution risk maps using disease occurrence and environmental data (45). Such models have the ability to extract associations between presence data (e.g., disease cases) and environmental variables, use those associations to characterize the environmental requirements for the disease agent, and subsequently deploy those associations to predict suitable geographic locations over non-sampled areas (12). This modeling approach has been commonly used to predict the geographic range of species in ecology (54) but has been used recently to model the distribution of diseases in both veterinary and human medicine (10,26,37,40,49,51,52,53). Arrays of mathematical algorithms currently used in ecological niche modeling include the use of machine-learning approaches (43). Combining the outputs of machine-learning methods with spatial clustering detection techniques (2,9,30) might provide a robust platform for guiding the design of surveillance systems in the ME.

Here, we tested whether a set of environmental and demographic variables can predict the geographic distribution of H5N1 HPAIV outbreaks reported in poultry holdings of the ME for the period 2005–14 using a presence-only maximum entropy ecological niche modeling method (Maxent). Furthermore, we assessed the spatiotemporal clustering of the disease in the ME for the same period of time using the scan statistic method. Combined results of both methodologies may shed further insights into the epidemiology of H5N1 HPAIV in the ME. Subsequently, these results may contribute to the formulation of surveillance programs that selectively target high-risk poultry areas, defined as highly probable suitable locations for the introduction, transmission, and maintenance of the disease, with specific demographic and environmental factors in the ME region.

MATERIALS AND METHODS

Data. *H5N1 HPAIV presence data.* Here, the term "Middle East (ME)" refers to countries of Southern and Western Asia and Northeastern Africa excluding Afghanistan, Pakistan, and India. Thus, the study region includes Turkey, Syria, Lebanon, Israel, Palestinian Territories, Jordan, Iraq, Iran, the countries of the Arabian Peninsula (Saudi Arabia, Yemen, Oman, United Arab Emirates, Qatar, Bahrain, Kuwait), Egypt, Libya, Sudan, Djibouti, Eritrea, and Somalia. Data used for this study were retrieved from the Food and Agriculture Organization of the United Nation (FAO) Global Animal Disease Information System EMPRES-i (18), which included geographic locations (Fig. 1) and dates of start of 3056 H5N1 HPAIV outbreaks reported by ME countries to the World Organization for Animal Health (OIE) from October 2005 to October 2014 in domesticated poultry holdings. Reported outbreaks, defined as the detection of one or more cases of the disease in an epidemiologic unit, where an epidemiologic unit was defined as a group of domesticated birds with a defined epidemiologic relationship that share approximately the same likelihood of exposure to the virus (41,42), were used as a proxy for disease presence.

Environmental data. Environmental variables (predictors) selected for this study were climate, global land cover, global poultry density, global livestock production system, and geographic locations of wetlands with >20,000 birds. Climate data were obtained from the WorldClim website (http://www.worldclim.org), a commonly used interpolated global climate data resource for ecological modeling and geographic information systems (24). WorldClim is a set of global climate data layers (climate grids) with a spatial resolution of 1, 5, 9, or 18 km. Variables included in the analysis were monthly mean, minimum and maximum temperature, monthly precipitation, and altitude. Those climatic data were further derived into a series of 19 bioclimatic variables. The WorldClim variables are smoothed maps of mean monthly climate data obtained from a variety of sources from 1950 through 2000. Data have been interpolated down to a 30 arc-second high-resolution grid, which is often referred to as "1 km^2" resolution. Owing to the large geographic range of the current study, only bioclimatic variables with an approximate spatial resolution of 9 km^2 were used to maintain the computation intensity of the model.

To provide an estimate of geographic representation of different land cover classes in the ME, global land cover use and livestock production systems data grids were obtained from the FAO web-based page on geo-spatial data, GeoNetwork (16,17). Data were available at an approximate spatial resolution of 5 km^2 and were categorized using an inventory of 11 and 14 classes for land cover use and livestock production systems, respectively.

Two demographic variables that are known to be associated with AI incidence in poultry, namely, geographic density of poultry and the geographic abundance of wild birds, were also included in the analysis. Global density of poultry was obtained from digital maps of approximate spatial resolution of 5 km^2 at FAO GeoNetwork Web page (15).

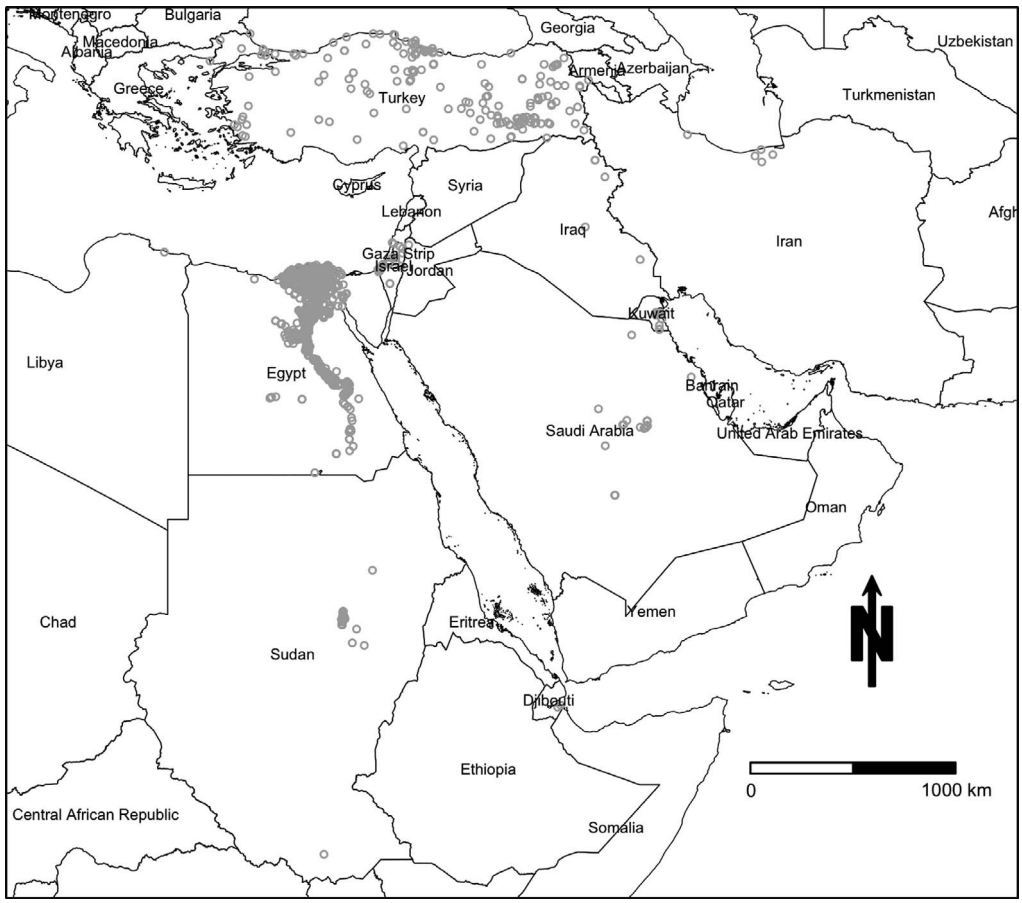

Fig. 1. Geographic locations of H5N1 highly pathogenic avian influenza outbreaks reported in poultry in the Middle East from October 2005 through October 2014.

Wetlands with more than 20,000 wild birds were obtained from the databases of two organizations for environmental conservation, namely, Convention on Wetlands of International Importance (RAMSAR) (56) and important bird areas (IBA) (6), which uses certain criteria as proxy for the location of wild water birds and has been used and described elsewhere (25,33,34,45). Because geographic abundance of wild birds was obtained as point data, variables were transformed into a smoothed kernel density grid layer with 5 km^2 spatial resolution and a search radius of 10 km^2 using ArcGIS version 10.1 (14). The choice of 5 km^2 spatial resolution for both variables ensured that the smoothed locations overlapped the geographic location of cells of the FAO poultry density grid, and, thus, both demographic layers will indirectly represent the spatial distribution of the population at risk. Thus, in total the number of variables evaluated in this study is equal to 28 environmental predictors, summarized in Table 1.

Environmental data layers were converted into a common projection and map extent using the Raster package (23) implemented in R statistical software version 3 (50). Furthermore, because the variables had different spatial scales (bioclimatic data ~9 km^2, global land cover ~250 m^2, FAO poultry density, wild birds abundance, and global livestock production systems ~5 km^2), they were aggregated and resampled to give them the same grid size, which resulted in a scale of approximately 11 km^2. Furthermore, colinearity in the environmental data was investigated by visually inspecting the relation between pairs of variables in scatter-plots.

Analytical methods. *Maxent Model.* The spatial risk for H5N1 HPAIV outbreaks was predicted using the presence-only maximum entropy ecological niche modeling technique (Maxent) (47). The Maxent program version 3.3.3, which was implemented as a function in the Dismo package (22) within the R software environment, was used for the analysis. A detailed description of the Maxent algorithm is available elsewhere (43,47). Briefly, Maxent operates by building ecological niche models to quantify the unknown probability of a distribution of a species (here, the population of H5N1 HPAIV-infected individuals) in a region, without inferring any unfounded information about the observed distribution. The algorithm identifies the distribution of the reported H5N1 HPAIV outbreaks that maximizes the predictions' entropy, which is either the most spread out distribution, or closest to uniform, under the null model. This is subject to a set of restrictions represented by the environmental parameters at a given location that represent the incomplete presence-only data information for the unknown potential locations of suitable places for H5N1 HPAIV outbreaks, when compared with the true distribution of the variable of interest. Those restrictions are the expected values of each environmental predictor, which should match its empirical average. In this study, the default convergence threshold, regularization, and number of iteration were selected, so that all models converged. In addition, the default logistic model was used, to ensure that predictions gave estimates between 0 and 1 for the risk of H5N1 HPAIV outbreak per map cell. Initially, independent Maxent models were fit for each of the 19 bioclimatic variables, as predictors for the disease in poultry, a procedure that resembles a bivariate analysis. Variables that had greater than 10% relative contribution in the prediction were included in the following subsequent, multivariable models, along with the above non-climatic demographic variables.

Maxent model performance evaluation. Performance of the Maxent model in predicting the spatial distribution of H5N1 HPAIV risk in poultry was evaluated using the threshold independent method. The method calculates the area under the curve (AUC) of the receiver operator characteristic (ROC). The AUC was calculated through a ROC plot of the sensitivity (the proportion of true predicted known presences, known as omission error) against 1 − specificity (proportion of false predicted known absences, known as commission error) over the whole range of threshold values between 0 and 1. The AUC value ranges from 0.5 and

compared the null model (entirely random predictive model) to a maximum value of 1 (perfectly discriminating predictive model). Maxent models with AUC > 0.75 for both training and testing data are usually considered accurate (13). The final model was selected using jackknife tests to calculate the contribution of each environmental variable to the model's prediction. Data were partitioned in two random sets (random sampling without replacement), for training and for testing purposes, respectively. The training set (training AUC) was used for model building, and the test set (testing AUC) was used to evaluate model accuracy using the value of the AUC. Because of the large geographic area analyzed in this study, a calibrated AUC (cAUC) was calculated for the final Maxent model to evaluate the extent of the spatial sorting bias (SSB) as suggested elsewhere (21). Here, the cAUC was used to assess the impact of countries with larger numbers of reported outbreaks on the predications of the final Maxent model (i.e., Egypt). If the cAUC value was close to 1, then one can conclude the absence of SSB (i.e., the large number of reported outbreaks in Egypt had a non-substantial impact on the predictions of the final Maxent model), while, if the value was close to zero, then SSB is present in the data. Furthermore, we repeated the analyses above twice to validate the accuracy of the selected environmental data in predicting the probability of the spatial distribution of H5N1 in the ME. Thus, our models all reported outbreaks in the ME (Model A); compromised only outbreaks reported in Egypt (Model B); and compromised outbreaks reported in the ME excluding Egypt (Model C). We compared the magnitude of change in the AUC values to further assess the sensitivity of the Maxent model to the reporting bias suffered by the presence data. Finally, pairwise Spearman correlation coefficients were calculated between each environmental variable and the predicted suitability of the outbreaks for the final Maxent model.

Space-time cluster analysis. Spatiotemporal clustering of H5N1 HPAIV outbreaks in the ME was modeled using the space-time permutation model of the scan statistic test implemented in the SaTScan software version 9.1 (31). A description of the scan statistic test, which has been broadly used in the assessment of animal disease clustering, is available elsewhere (2,3,30,32,57). The model was run using only outbreak location and starting date under the null hypothesis that outbreaks were randomly distributed in space and time. The model was set to scan for areas with high case numbers or infection rates, so that they test for clusters with a spatial and temporal occurrence that is higher than that outside the cluster. The maximum size of the temporal window was set to 6 months, which represents the maximum duration of surveillance activities during the onset of the first case in most Middle Eastern countries during the 2005–07 epidemic wave. The maximum spatial extension of clusters was set to a radius of 50 km, based on the average size of the administrative areas in the Middle East. Finally, time aggregation was set to 7 days, to avoid "Monday effect" (i.e., the bias introduced due to underreporting over the weekends), because the extension of weekends vary in ME countries, depending on cultural and religious factors, and because identification of risk periods in terms of weeks, rather than days, was considered sufficiently accurate for surveillance purposes. Distributions of the likelihood ratio and its corresponding P value were obtained using Monte Carlo simulation by generating 999 replications of the data set under the null hypothesis of random distribution of cases in time and space. The test statistics were computed for each random replication, as well as for the HPAIV H5N1 dataset, and if the latter was in the most extreme 5% of all test statistics calculated, then the hypothesis test was deemed significant at $P = 0.05$.

RESULTS

Prevalence of H5N1 HPAIV was substantially greater in Egypt, followed by Sudan and Turkey, whereas prevalence in other ME countries did not exceed 1% (Fig. 2A). Like the rest of the Eurasian countries, most of the detected outbreaks were reported in 2006 in ME countries (Fig. 3). However, Egypt had another high incidence of outbreaks reported between 2010 and 2011, so that, in total, Egypt accounted for more than 80% of the outbreaks reported in the region (Fig. 2B).

Only four of the selected environmental variables were needed to adequately predict the geographic distribution of H5N1 outbreaks in the ME with an AUC higher than 0.75 and a cAUC substantially closer to 1 than 0 (Table 1). The final Maxent models included precipitation of the warmest quarter, global livestock production systems, global poultry density, and mean temperature of the warmest quarter (Table 2). Both global land cover and geographic abundance of wild water birds contributed least to the prediction of the model (relative contribution $<5\%$), and they did not improve the value of the AUC or the cAUC for the test data (Table 2). However, based on the validation procedure to assess adequacy of the environmental variables in predicting the spatial risk of H5N1 in the ME, the results indicate that precipitation of the warmest quarter and global poultry density were the most important environmental predictors in Egypt, whereas global livestock production systems and mean temperature of the warmest quarter were the most important environmental predictors in other countries (Table 2). No substantial changes were observed in the AUC values for any of the Maxent models (Table 2).

The predicted spatial risk (or suitability) for H5N1 in poultry in the ME is shown in Fig. 3. Most of the ME countries were predicted as suitable areas for H5N1 HPAIV. However, the highest risk areas (>0.8) were primarily distributed across the Nile delta and valley in Egypt, followed by Palestinian Territories, northwestern Syria, and small parts of northeastern portions of the Arabian Peninsula (>0.6). Furthermore, the risk maps for the three Maxent models were relatively consistent in predicting the spatial risk of H5N1 HPAIV in the region (Fig. 3).

Based on the results of the final Maxent model and Spearman's correlation (Tables 2 and 3), geographic regions with approximate mean precipitation greater than 0 mm, which ranged between 0 (minimum) and 65 mm (maximum) in the ME in the warmest quarter of the year, were found most suitable for the risk of introduction of H5N1 HPAIV in poultry (<0.6). Urban and mixed irrigated hyper arid livestock production areas and geographic regions with the lowest poultry population density were also found most suitable (<0.7). Finally, geographic regions with approximate mean temperatures lower than 35 C, which ranged between 25.4 C (minimum) and 38.9 C (maximum) in the warmest quarter of the year, were found most suitable for H5N1 in the ME.

The results of the space-time permutation model of the scan statistic analysis showed 23 most likely clusters ($P < 0.001$) of H5N1 HPAIV outbreaks in the ME between 2005 and 2014 (Fig. 4). Fifteen spatiotemporal clustering events were detected in the Nile delta and valley in Egypt (Fig. 4A) with spatial extensions ranging between 0 and 49.5 km radius, and temporal duration ranging between 26 and 1221 days (Fig. 4B). Four clustering events were detected in Turkey, two in Saudi Arabia, and one each in Kuwait and Sudan (Fig. 4A). Fig. 4A also demonstrates the combined results of the final Maxent model and space-time cluster analysis.

DISCUSSION

We used an ecological niche modeling approach based on outbreak presence-only data to, first, estimate the potential spatial distribution of H5N1 HPAIV outbreaks in poultry the ME and the environmental factors underlying to that pattern, and, second, to investigate the magnitude of spatial and temporal clustering of those outbreaks in the region. In this study, the role of environmental variables in the development of an ecological niche for H5N1 HPAIV in poultry was investigated independently of country boundaries by creating a

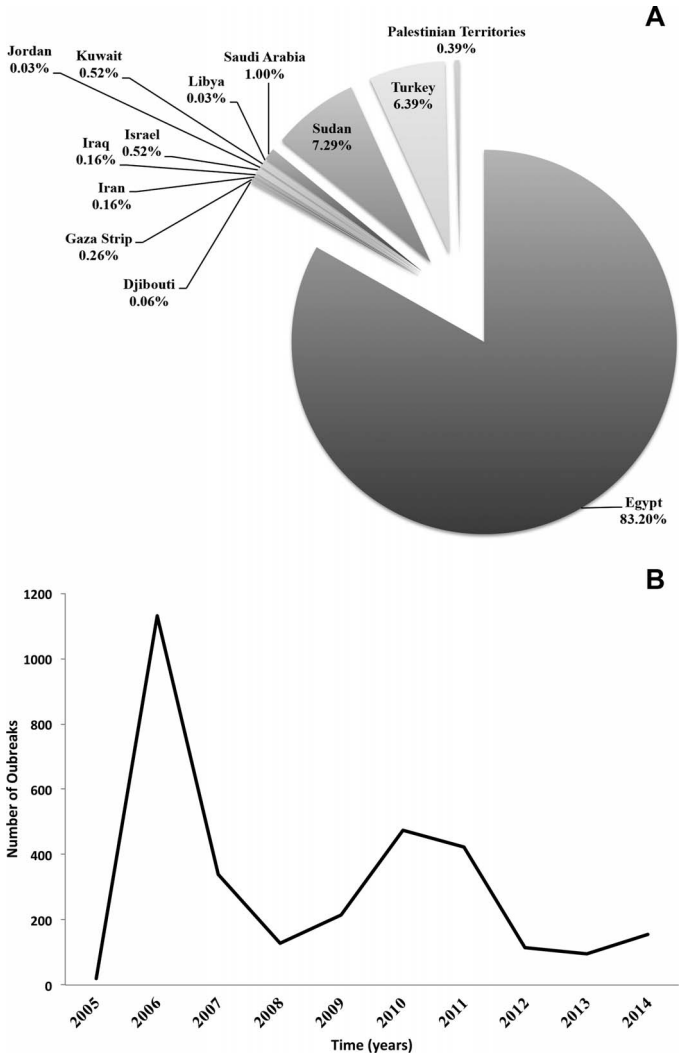

Fig. 2. (A) Prevalence of H5N1 HPAI outbreaks (per country) in poultry in the Middle East between 2005 and 2014. (B) Temporal distribution of H5N1 HPAI outbreaks (per year) in poultry in the Middle East from October 2005 through October 2014.

regional scale model. Generally, our findings are consistent with earlier studies aimed at predicting the ecological niche of H5N1 in the ME region (19,58,59). During the 2005–14 period, the highest prevalence of H5N1 HPAIV in poultry in the ME was reported in the Nile delta and valley of Egypt (Figs. 1 and 2A), and, therefore, Egypt was predicted as the highest risk area for the disease (Fig. 3). However, the inclusion of the present set of environmental variables into the Maxent model resulted in finding the Palestinian Territories, northwestern Syria, and small parts of northeastern Arabia (Fig. 3) to be high-risk areas with conditions suitable for the introduction of H5N1 HPAIV in their poultry populations. Hence, based on the importance of the selected environmental variables in predicting H5N1 HPAIV outbreaks, geographic regions or countries with few or no reported outbreaks could still be predicted as high-risk areas if the climatic conditions and demographics are suitable for the introduction of the disease. Results of the presence-only Maxent approach produced a robust ecological niche model for H5N1 HPAIV (Table 2) and demonstrated that the environmental variables included in this study were adequate predictors for the outbreaks in poultry in the ME.

Out of the 19 bioclimatic variables, precipitation and mean temperature of the warmest quarters were the most important bioclimatic predictors of H5N1 HPAIV in poultry. The correlation of both climatic variables (Table 3) to the predicted suitability of H5N1 in poultry in the ME region suggests that geographic areas with precipitation greater than 0 mm and lower temperatures than 35 C in the warmest quarters are high-risk areas for virus introduction. Indeed, Egypt, Syria, Palestinian Territories, and Israel have the lowest temperatures with occasional minimal rainfall during the summer, when compared with other countries of the Arabian Peninsula. This result is consistent with the notion that regions with seasons of low annual rainfall and low temperatures could be identified as high-risk areas for AI virus outbreaks (19). Furthermore, human H5N1 outbreaks had been highly associated with outbreaks in poultry due to frequent human-poultry contact, especially in Egypt (28), it has been suggested that this is mainly attributed to human activities influenced by climatic conditions, for example farming practices or swimming in ponds that poultry use (35). Thus, such factors have to be properly studied to shed further insight on the relationship between climatic conditions and transmission patterns of H5N1 HPAIV between human and poultry (28,35).

As expected, urban and mixed irrigated hyper arid livestock production areas were suitable locations for H5N1 introduction because the former is common in Egypt and Sudan, whereas the latter is common in other ME countries (e.g., Arabian Peninsula). Here, hyper arid areas are defined by the FAO as areas with zero growing days (16) and characterized by extremely dry climate. The mixed irrigated hyper arid system is composed of low animal density sited in large geographic areas across the densely populated Nile delta and valley, leading to large livestock biomass, and subsequently provides favorable conditions for transmission and persistence of H5N1 in poultry (5). Backyard poultry holdings are also common in urban livestock production systems in ME countries, which are well known as suitable land classes for H5N1 HPAIV transmission (48,59). Furthermore, urban production systems are under intensive human surveillance, and thus the number of detected outbreaks is expected to be higher than nonurban production systems. The results of the study here suggest that predicted risk for H5N1 HPAIV in poultry was high near geographic regions with low poultry population density in the ME. This is not surprising given that most poultry cases were detected in either backyard poultry holdings, or small poultry holdings with low biosecurity measures, which constitute ideal environments for the transmission and circulation of AI infection. In addition, backyard poultry holdings are more commonly exposed to frequent human contact than large commercial poultry farms, and, therefore, they might constitute an ideal environment for viral transmission and maintenance. This is important because it might be associated with the high prevalence of H5N1 HPAIV human cases in Egypt, in which most of the detected cases were in contact with backyard poultry (34). Thus, inclusion of information related to holding characteristics, such as biosecurity level, size, type of production, and species, might substantially improve the prediction of the presented model. Most important, the use of the poultry density raster alone to guide the allocation of resources for surveillance may be misleading. We believe that the main reason for the insignificant role of global land cover in predicting the risk of H5N1 in the ME is that both global livestock production systems and poultry density provided sufficient predictive ability (as demographic variables) to our presented model.

Our model suggested that geographic proximity of poultry holdings to wetlands abundant with wild aquatic birds has no significant role in the introduction or persistence of H5N1 HPAIV in the ME

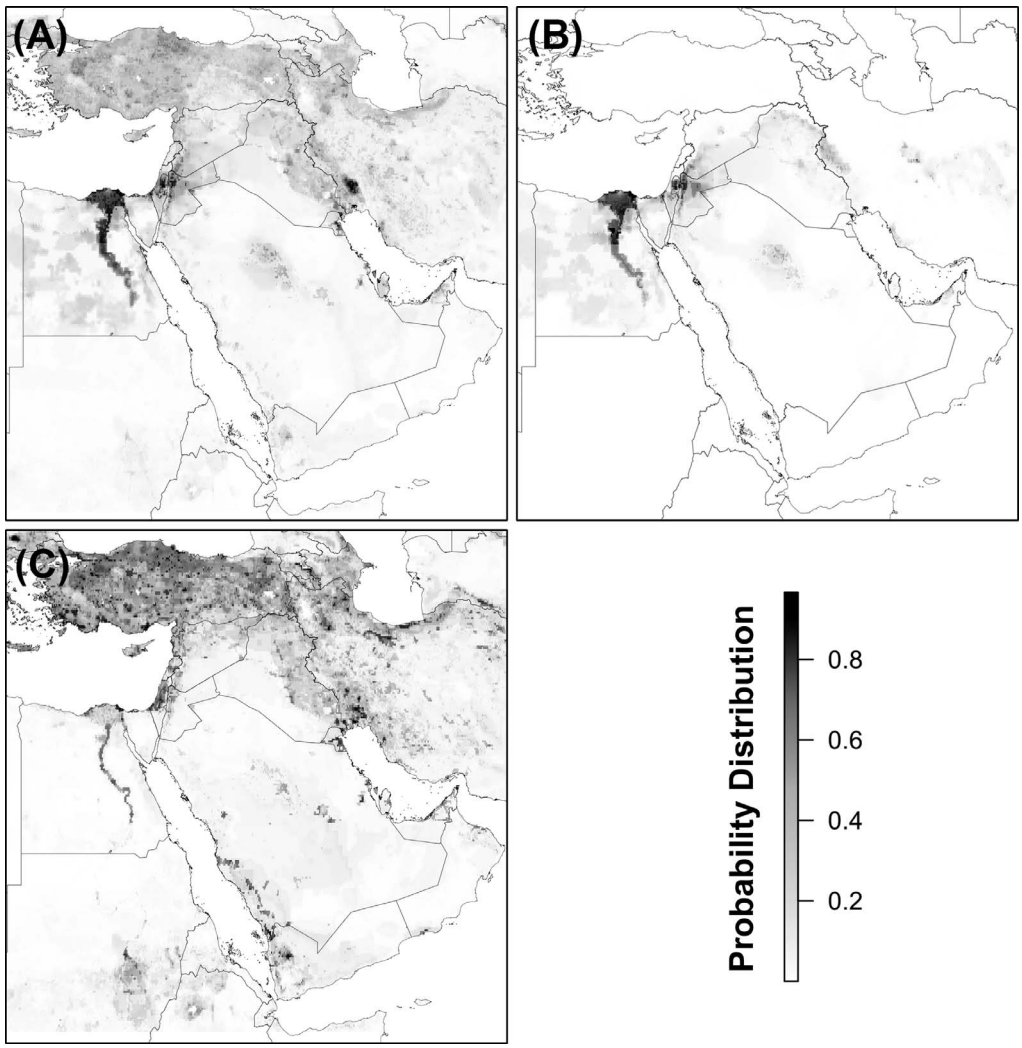

Fig. 3. Predicted probability distribution for the geographic risk for H5N1 HPAI in poultry in the Middle East from October 2005 through October 2014. (A) Maxent model for all reported outbreaks data; (B) Maxent model for outbreaks data reported in Egypt only; (C) Maxent model for all reported outbreaks data excluding Egypt.

region. Although the ME is seated on important wild bird migration routes, the inland water surfaces, which are considered the most important habitat for wild aquatic birds in the region, are scarce when compared to the Americas, Europe, or Southeast Asia. Hence, as suggested elsewhere (46), the ME region has indeed a much lower risk for H5N1 HPAIV introduction from wild birds (19), which also explains the extremely low prevalence of detected wild bird cases. Furthermore, during the peak of the epidemic in 2005–07, ME countries intensified their surveillance efforts on domesticated poultry holdings, whereas few countries mobilized their resources toward wild bird surveillance, which is arguably due to the lack of sufficient resources, when compared, for example, with European countries.

The permutation model of the scan statistic test identified 23 significant spatiotemporal clusters of H5N1 HPAIV outbreaks centered mainly in Egypt, followed by Turkey, Saudi Arabia, Sudan, and Kuwait (Fig. 4), for which the prevalence of HPAIV H5N1 cases was higher than that expected if cases were randomly distributed throughout the area under study. Most of the detected clusters in the ME region were centered either in agricultural areas or in close proximity to major cities. Furthermore, most of the cases within each significant cluster were either detected in backyard or medium size (<1000) poultry holdings, which are characterized by very low to medium biosecurity measures. Results suggest strong seasonal variation for the risk of H5N1 HPAIV in the ME (Fig. 4). The temporal dimension of the clusters detected in Turkey, Kuwait, and Saudi Arabia suggests that winter and spring are indeed the most important periods of time for clustering of H5N1 HPAIV. However, some of the clusters detected in Egypt, in addition to the one detected in Sudan, suggest that summer and fall were also high-risk periods of time for clustering of H5N1 HPAIV, which is reflected in the inflated temporal duration of some Egyptian clusters (2–3 years).

One of the most interesting findings of the present study is that all of the identified clusters encompassed moderate to high-risk (probabilities between 0.8 and 0.4) suitable areas for H5N1 HPAIV predicted by the Maxent model. This indeed confirms the notion that the underlying environmental and demographic variables were suitable for H5N1 HPAIV clustering, transmission, circulation, and persistence. Those factors are mostly prominent in Egypt, which might further explain the reason that it is the sole H5N1 HPAIV epicenter for the Middle East. The temporal dimension of the significant spatiotemporal clusters suggests that winter and spring were the most likely periods of time for the occurrence of H5N1 HPAIV in Turkey, Saudi Arabia, and Kuwait between 2006 and 2007. However, the temporal overlap between the climatic predictors of the present

Table 1. Data sources and properties of the environmental variables used to model the probability of spatial distribution of H5N1 highly pathogenic avian influenza outbreaks reported in the Middle East. Spatial resolution is 5 km^2 for all sources.

ID	Source	Type	Time period	Spatial resolution
1	WorldClim Global	Minimum temperature	1950–2000	9 km^2
2	Climate Data	Maximum temperature		9 km^2
3		Mean temperature		9 km^2
4		Precipitation		9 km^2
5		Altitude		9 km^2
6		BIO1 = annual mean temperature		9 km^2
7		BIO2 = mean diurnal range (mean of monthly (max temp − min temp))		9 km^2
8		BIO3 = isothermality (BIO2/BIO7 * 100)		9 km^2
9		BIO4 = temperature seasonality (standard deviation *100)		9 km^2
10		BIO5 = max temperature of warmest month		9 km^2
11		BIO6 = min temperature of coldest month		9 km^2
12		BIO7 = temperature annual range (BIO5–BIO6)		9 km^2
13		BIO8 = mean temperature of wettest quarter		9 km^2
14		BIO9 = mean temperature of driest quarter		9 km^2
15		BIO10 = mean temperature of warmest quarter		9 km^2
16		BIO11 = mean temperature of coldest quarter		9 km^2
17		BIO12 = annual precipitation		9 km^2
18		BIO13 = precipitation of wettest month		9 km^2
19		BIO14 = precipitation of driest month		9 km^2
20		BIO15 = precipitation seasonality (coefficient of variation)		9 km^2
21		BIO16 = precipitation of wettest quarter		9 km^2
22		BIO17 = precipitation of driest quarter		9 km^2
23		BIO18 = precipitation of warmest quarter		9 km^2
24		BIO19 = precipitation of coldest quarter		9 km^2
25	FAO GeoNetwork	Global poultry density	2005	5 km^2
26		Livestock production systems with 14 discrete spatial features	2011	5 km^2
27		Global land cover distribution, by dominant land cover type with 11 discrete spatial features	2007	250 m^2
28	RAMSAR and IBAs	Kernel density raster for wetlands with more than 20,000 wild birds	2014	5 km^2

Maxent model and most of the space-time clusters detected in the Nile delta and valley suggests that weather conditions had an important role in the persistence of H5N1 HPAIV outbreaks in Egypt. However, the fact that summer temperatures in the Arabian Peninsula always exceed 35 C indicates that poultry holding demographics (type of production system and poultry density) play a more important role in predicting the risk of H5N1 HPAIV outbreak in poultry than climate, as suggested elsewhere (58,59). This is because the clusters detected in Kuwait and Saudi Arabia encompassed outbreaks reported either in backyard or medium sized poultry holdings located either in urban areas or in close proximity to urban areas.

Table 2. Estimates of the relative contributions of the environmental variables to the Final Maxent models and their validation AUC values for predicting the risk of H5N1 highly pathogenic avian influenza outbreaks in poultry in the Middle East. Model A, the use of all reported outbreaks data; Model B, the use of outbreaks data reported in Egypt only; Model C, the use of all reported outbreaks data excluding Egypt.

Variable	Percentage contribution	AUC for training data	AUC for test data	Calibrated AUC for test data
Model A				
Precipitation of the warmest quarter	47.2	0.90	0.96	0.73
Global livestock production systems	18.1			
Global poultry density	16.7			
Mean temperature of the warmest quarter	13.3			
Wetlands abundant with wild birds	3.8			
Land cover	0.9			
Model B				
Precipitation of the warmest quarter	36.6	0.97	0.95	0.79
Global poultry density	29.6			
Mean temperature of the warmest quarter	14.8			
Global livestock production systems	14.7			
Wetlands abundant with wild birds	4.3			
Land cover	0			
Model C				
Global livestock production systems	36.1	0.94	0.95	0.78
Mean temperature of the warmest quarter	26.4			
Global poultry density	14.5			
Precipitation of the warmest quarter	13.2			
Land cover	4.5			
Wetlands abundant with wild birds	2.3			

Table 3. Spearman correlation coefficients between each environmental variable and the predicted suitability of H5N1 HPAI outbreaks in poultry in the Middle East.

	Geographic distribution of HPAI in poultry
Precipitation of the warmest quarter	−0.57
FAO global livestock production systems	0.39
FAO poultry density	−0.66
Mean temperature of the warmest quarter	−0.19
Wetlands abundant with wild birds	0.12

Accuracy of the environmental and demographic variables in predicting the presence of the outbreaks might be substantially improved with sufficiently higher resolution datasets across the study region. Using environmental data with different spatial resolutions (higher or lower than the present study) might result in completely different Maxent models and/or might affect the value of the percentage contribution of each environmental predicator in each resulting Maxent model (4). However, a study suggested that the ecological niche of H5N1 HPAIV outbreaks can be adequately predicted on regional levels using environmental data layers, similar to the current study setting, with spatial resolution of up to 10 km^2 (58). Furthermore, tranportation of live poultry has been heavily implicated in the transmission and maintanance of HPAIV in South Asia (53), and, therefore, the inclusion of land cover data grids for the ME with more detailed features that represent, for example, railroads and motorways, would substantially improve the prediction of the presented model.

Accuracy and representativeness of the information collected has an essential impact on the epidemiological investigation of disease outbreaks and on model prediction. A study aiming to investigate space-time clustering of H5N1 HPAIV in wild birds has demonstrated how the inclusion of information on the locations of negative samples could result in different space-time clusters, when compared with the use of information on the locations of positive samples alone (2). Furthermore, it has been shown that the prediction of machine-learning methods can be substantially improved when including AI negative samples in such models (19). Here, information on the locations of negative samples was not available; therefore, the Maxent model was used to simulate pseudo absence data (negative samples), which are drawn purely at random from the study region (47). However, since pseudo absence data do not represent true absences of the disease, it may lead to mis-predicting a known presence, which might be a limitation of the predictions here. Although reporting of H5N1 HPAIV is mandatory for OIE member countries, this mandate does not necessarily imply that every case or outbreak has been reported, arguably, because of substantial differences in the surveillance capabilities between the ME countries. For that reason, presence data used in

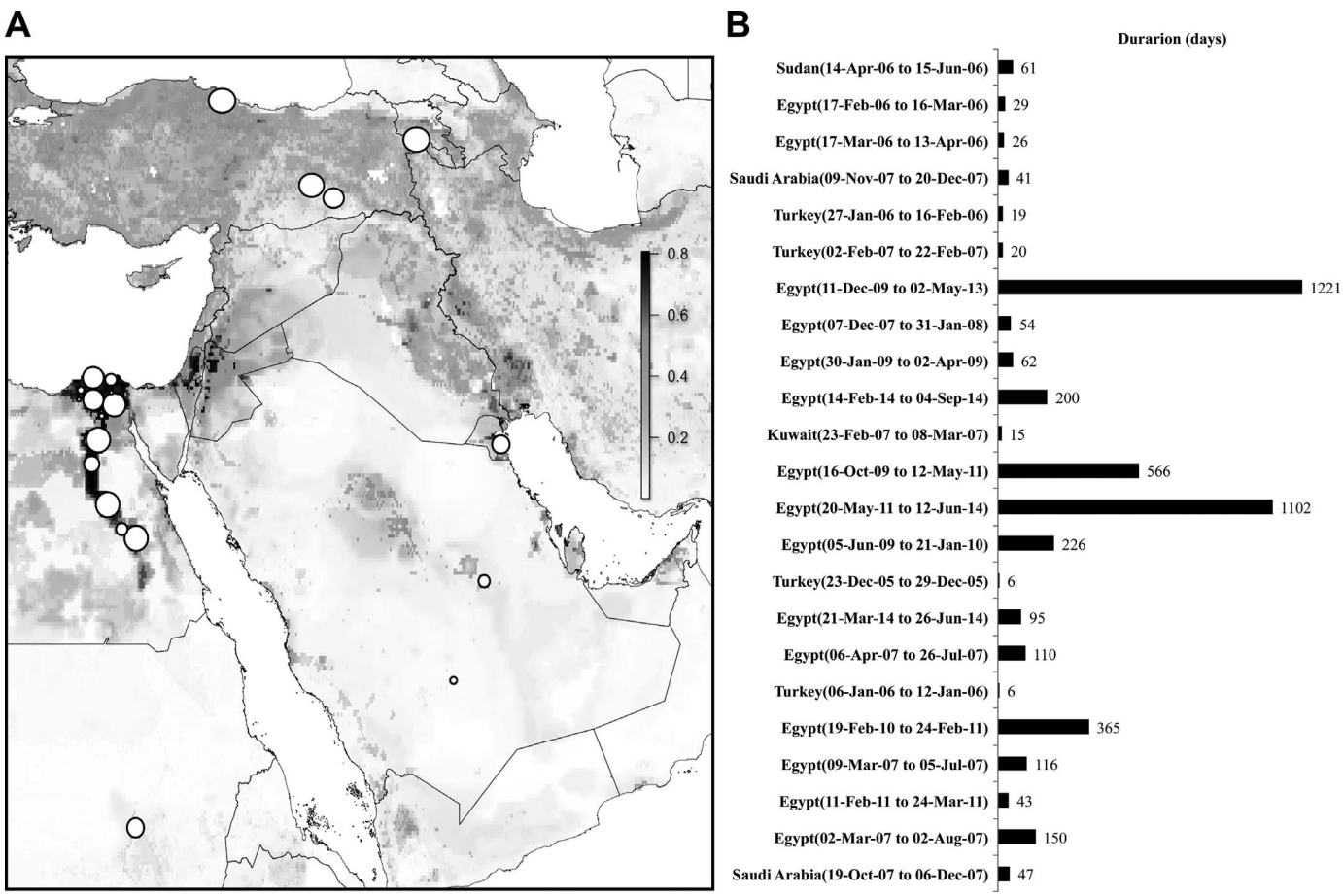

Fig. 4. Combined results of the permutation model of the scan statistics and presence-only maximum entropy ecological niche model for H5N1 HPAIV in poultry in the Middle East from October 2005 through October 2014. (A) Locations of top 23 HPAIV H5N1 most likely spatiotemporal clusters ($P < 0.001$) as detected by permutation scan statistic overlapped on the results of the Maxent model. The radius (km) of the white circles is relative to the predicted spatial extent of a given cluster. (B) Temporal duration (in days) for the top 23 most likely spatiotemporal clusters. The temporal extension of each cluster is ordered from up (as the 1st most likely cluster) to down (as the 23rd most likely cluster) for each country.

the study here may have been biased toward geographic regions in ME with higher surveillance capabilities, leading to predictions skewed toward these countries. Furthermore, geographic regions in the ME with poorer surveillance capabilities might have been underrepresented (i.e., inaccurately represented) in the selected environmental layers, and therefore, the predicted risk of H5N1 HPAIV in those countries has been diluted toward the null. That said, the use of environmental, demographic, and spatial data with machine-learning methods may, at least in part, compensate that bias, because predictions are based on the correlation between predictors and disease, mostly, in areas with a high concentration of data available, which is then used to predict risk in areas in which incidence data may be scarce. This notion has been confirmed by our sensitivity analysis (Table 2), in which removing the Egyptian outbreaks did not lead to a drastic drop in the values of AUCs, specifically the conservative cAUC, and, interestingly, the risk map of Maxent model C continued to identify the Egyptian part of the Nile valley as a high-risk area (Fig. 3C). Furthermore, our procedure led, for example, to identifying high-risk areas in Syria, despite the limited reporting of H5N1 HPAIV cases available from that country. However, the resulting risk maps for the relative probability of H5N1 HPAIV occurrence are not definitive and need to be updated periodically. Furthermore, the model predictions suggest that the reason that some ME countries did not report cases of H5N1 HPAIV (e.g., Qatar and United Arab Emirates) might simply be that they did not exhibit suitable environmental conditions for the emergence of H5N1 HPAIV in their poultry populations. Subsequently, an additional use of the Maxent prediction here may be as a proxy for the distinction between geographic areas in which absence of reporting was likely due to a true absence of disease (such as those suggested for Qatar or the United Arab Emirates) from those in which disease may have gone underreported (such as some parts of Syria).

In conclusion, high-risk geographic areas and periods of time, with their underlying environmental and demographic factors, for the introduction and circulation of H5N1 HPAIV in poultry in the ME between 2005 and 2014 were identified. Results suggest that more information related to poultry holding demographics is needed to further improve the risk prediction for H5N1 HPAIV in the ME, whereas the methodology presented here may be useful in guiding the design of surveillance programs and in identifying areas in which underreporting may have occurred.

REFERENCES

1. Abdelwhab, E. M., and H. M. Hafez. An overview of the epidemic of highly pathogenic H5N1 avian influenza virus in Egypt: epidemiology and control challenges. Epidemiol. Infect. 139:647–657. 2011.

2. Alkhamis, M., P. Willeberg, U. Carlsson, T. Carpenter, and A. Perez. Alternative scan-based approaches to identify space-time clusters of highly pathogenic avian influenza virus H5N1 in wild birds in Denmark and Sweden in 2006. Avian Dis. 56:1040–1048. 2012.

3. Alkhamis, M. A., A. M. Perez, H. Yadin, and N. J. Knowles. Temporospatial clustering of foot-and-mouth disease outbreaks in Israel and Palestine, 2006–2007. Transbound Emerg. Dis. 56:99–107. 2009.

4. Atkinson, P. M., and A. J. Graham. Issues of scale and uncertainty in the global remote sensing of disease. Adv. Parasitol. 62:79–118. 2006.

5. Awulachew, S. B., D. Molden, and D. Peden. Livestock and water in the Nile River Basin. In: The Nile River basin: water, agriculture, governance and livelihoods. D. Molden and S. B. Awulachew, eds. Routledge, London. 2012.

6. Bird Life International. Important bird areas database. [2007; accessed 2016 Jan 21]. Available from: http://www.birdlife.org/datazone/home

7. Breed, A. C., K. Harris, U. Hesterberg, G. Gould, B. Z. Londt, I. H. Brown, and A. J. Cook. Surveillance for avian influenza in wild birds in the European Union in 2007. Avian Dis. 54:399–404. 2010.

8. Brown, I. H., M. Pittman, V. Irza, and A. Laddomada. Experiences in control of avian influenza in Europe, the Russian Federation and the Middle East. Dev. Biol. (Basel) 130:33–38. 2007.

9. Carpenter, T. E. Methods to investigate spatial and temporal clustering in veterinary epidemiology. Prev. Vet. Med. 48:303–320. 2001.

10. Chikerema, S. M., A. Murwira, G. Matope, and D. M. Pfukenyi. Spatial modelling of *Bacillus anthracis* ecological niche in Zimbabwe. Prev. Vet. Med. 111:25–30. 2013.

11. Delgado, C. L. Rising consumption of meat and milk in developing countries has created a new food revolution. J. Nutr. 133: 3907s–3910s. 2003.

12. Elith, J., and J. R. Leathwick. Species distribution models: ecological explanation and prediction across space and time. Annu. Rev. Ecol. Evol. S 40:677–697. 2009.

13. Elith, J. H., C. P. Graham, R. Anderson, M. DudÌk, S. Ferrier, A. J. Guisan, R. Hijmans, F. R. Huettmann, J. Leathwick, A. Lehmann, J. G. Li, L. A. Lohmann, B. Loiselle, G. Manion, C. Moritz, M. Nakamura, Y. Nakazawa, J Overton, P. A. Townsend, S. Phillips, K. Richardson, R. E. Scachetti-Pereira, R. Schapire, J. Soberûn, S. S. Williams, M. E. Wisz, and N. Zimmermann. Novel methods improve prediction of species distributions from occurrence data. ECOG 29:129–151. 2006.

14. [ESRI] Environmental Systems Research Institute. ArcGIS Desktop, 10.1 ed. Environmental Systems Research Institute, Redlands, CA. 2012.

15. [FAO] Food and Agricultural Organization of the United Nations. FAO Geonetwork. Global Poultry Density. [2005; accessed 2016 Jan 21]. Available from: http://www.fao.org/ag/againfo/resources/en/glw/GLW_dens.html

16. FAO. Food and Agricultural Organization Geonetwork. Global land cover distribution, by dominant land cover type by H. von Velthuizen et al. [2007; accessed 2014 Sep]. Available online: http://data.fao.org/map?entryId=b915a4c0-7592-11db-b9b2-000d939bc5d8

17. FAO. Food and Agricultural Organization Geonetwork. Global Livestock Production Systems. [2011; accessed 2016 Jan 21]. Available from: http://www.fao.org/docrep/014/i2414e/i2414e00.htm

18. FAO. Food and Agriculture Organization (FAO). EMPRES Global Animal Disease Information System (EMPRES-i). [2014; accessed 2016 Jan 21]. Available from: http://empres-i.fao.org/

19. Herrick, K. A., F. Huettmann, and M. A. Lindgren. A global model of avian influenza prediction in wild birds: the importance of northern regions. Vet. Res. 44:42. 2013.

20. Hesterberg U., K. Harris, A. Cook, and I. Brown. Annual Report of the EU Avian Influenza Surveillance in Wild Birds 2006. In: Surveillance for avian influenza in wild birds carried out by member states, February–December 2006. European Commission, Health & Consumer Protection directorate-General. [revised 2007; accessed 2016 Jan 21]. Available from: http://ec.europa.eu/food/animal/diseases/controlmeasures/avian/eu_resp_surveillance_en.htm

21. Hijmans, R. J. Cross-validation of species distribution models: removing spatial sorting bias and calibration with a null model. Ecology 93:679–688. 2012.

22. Hijmans, R. J. Dismo: Species distribution modeling, Davis, CA. [2013; accessed 2016 Jan 21]. Available from: http://cran.r-project.org/web/packages/dismo/vignettes/sdm.pdf

23. Hijmans, R. J. Raster: Geographic data analysis and modeling, Davis, CA. [2013; accessed 2016 Jan 21]. Available from: http://cran.r-project.org/web/packages/raster/raster.pdf

24. Hijmans, R. J., S. E. Cameron, J. L. Parra, P. G. Jones, and A. Jarvis. Very high resolution interpolated climate surfaces for global land areas. J. Climatol. 25:1965–1978. 2005.

25. Iglesias, I., M. Jesus Munoz, M. Martinez, and A. de la Torre. Environmental risk factors associated with H5N1 HPAI in Ramsar wetlands of Europe. Avian Dis. 54:814–820. 2010.

26. Illoldi-Rangel, P., C. L. Rivaldi, B. Sissel, R. Trout Fryxell, G. Gordillo-Perez, A. Rodriguez-Moreno, P. Williamson, G. Montiel-Parra, V. Sanchez-Cordero, and S. Sarkar. Species distribution models and ecological suitability analysis for potential tick vectors of lyme disease in Mexico. J. Trop. Med. 2012:959101. 2012.

27. Jones, K. E., N. G. Patel, M. A. Levy, A. Storeygard, D. Balk, J. L. Gittleman, and P. Daszak. Global trends in emerging infectious diseases. Nature 451:990–993. 2008.

28. Kayali, G., R. J. Webby, M. F. Ducatez, R. A. El Shesheny, A. M. Kandeil, E. A. Govorkova, A. Mostafa, and M. A. Ali. The epidemiological and molecular aspects of influenza H5N1 viruses at the human-animal interface in Egypt. PLoS One 6:e17730. 2011.

29. Kovats, R. S., D. H. Campbell-Lendrum, A. J. McMichael, A. Woodward, and J. S. Cox. Early effects of climate change: do they include changes in vector-borne disease? Philos. Trans. R. Soc. B: Biol. Sci. 356: 1057–1068. 2001.

30. Kulldorff, M., R. Heffernan, J. Hartman, R. Assuncao, and F. Mostashari. A space-time permutation scan statistic for disease outbreak detection. PLoS Med. 2:e59. 2005.

31. Kulldorff, M. and Information Management Services Inc. SatScan v9.1.1: Software for the spatial and space-time scan statistics. [2012; accessed 2016 Jan 21]. Available from: http://www.satscan.org

32. Kulldorff, M., and N. Nagarwalla. Spatial disease clusters: detection and inference. Stat. Med. 14:799–810. 1995.

33. Martinez, M., M. J. Munoz, A. De La Torre, I. Iglesias, S. Peris, O. Infante, and J. M. Sanchez-Vizcaino. Risk of introduction of H5N1 HPAI from Europe to Spain by wild water birds in autumn. Transbound Emerg. Dis. 56:86–98. 2009.

34. Martinez, M., A. M. Perez, A. de la Torre, I. Iglesias, and M. J. Munoz. Association between number of wild birds sampled for identification of H5N1 avian influenza virus and incidence of the disease in the European Union. Transbound Emerg. Dis. 55:393–403. 2008.

35. Mathur, M. B., R. B. Patel, M. Gould, T. M. Uyeki, J. Bhattacharya, Y. Xiao, Y. Gillaspie, C. Chae, and N. Khazeni. Seasonal patterns in human A (H5N1) virus infection: analysis of global cases. PLoS One 9:e106171. 2014.

36. McMichael, A. J., R. E. Woodruff, and S. Hales. Climate change and human health: present and future risks. Lancet 367:859–869. 2006.

37. Mischler, P., M. Kearney, J. C. McCarroll, R. G. Scholte, P. Vounatsou, and J. B. Malone. Environmental and socio-economic risk modelling for Chagas disease in Bolivia. Geospat. Health 6:S59–66. 2012.

38. Mukhtar, M. M., S. T. Rasool, D. Song, C. Zhu, Q. Hao, Y. Zhu, and J. Wu. Origin of highly pathogenic H5N1 avian influenza virus in China and genetic characterization of donor and recipient viruses. J. Gen. Virol. 88:3094–3099. 2007.

39. Munster, V. J., C. Baas, P. Lexmond, J. Waldenström, A. Wallensten, T. Fransson, G. F. Rimmelzwaan, W. E. P. Beyer, M. Schutten, B. R. Olsen, A. D. M. E. Osterhaus, and R. A. M. Fouchier. Spatial, temporal, and species variation in prevalence of influenza A viruses in wild migratory birds. PLoS Pathogens 3:e61. 2007.

40. Nogareda, C., A. Jubert, V. Kantzoura, M. K. Kouam, H. Feidas, and G. Theodoropoulos. Geographical distribution modelling for *Neospora caninum* and *Coxiella burnetii* infections in dairy cattle farms in northeastern Spain. Epidemiol. Infect. 141:81–90. 2013.

41. [OIE] World Organisation for Animal Health. Terrestrial Animal Health Code 23rd Edition, [2014; accessed 2016 Jan 21]. Available from: http://www.oie.int/international-standard-setting/terrestrial-code/

42. OIE. World Animal Health Information Database (WAHID) Interface. [2014; accessed 2016 Feb 1]. Available from: http://www.oie.int/wahis_2/public/wahid.php/Diseaseinformation/WI

43. Olden, J., D. Lawler, J. Joshua, N. Poff, L. Roy. machine learning methods without tears: a primer for ecologists. Q. Rev. Biol. 83: 171–193. 2008.

44. Ottaviani, D., S. de la Rocque, S. Khomenko, M. Gilbert, S. H. Newman, B. Roche, K. Schwabenbauer, J. Pinto, T. P. Robinson, and J. Slingenbergh. The cold European winter of 2005–2006 assisted the spread and persistence of H5N1 influenza virus in wild birds. Ecohealth 7:226–236. 2010.

45. Peterson, A. T., J. T. Bauer, and J. N. Mills. Ecologic and geographic distribution of filovirus disease. Emerg. Infect. Dis. 10:40–47. 2004.

46. Pfeiffer, D. U. Assessment of H5N1 HPAI risk and the importance of wild birds. J. Wildlife Dis. 43:S47–S50. 2007.

47. Phillips, S. J., R. P. Anderson, and R. E. Schapire. Maximum entropy modeling of species geographic distributions. Ecol. Model. 190:231–259. 2006.

48. Prosser, D. J., L. L. Hungerford, R. M. Erwin, M. A. Ottinger, J. Y. Takekawa, and E. C. Ellis. Mapping avian influenza transmission risk at the interface of domestic poultry and wild birds. Frontiers Public Health 1:28. 2013.

49. Quintana, M., O. Salomon, R. Guerra, M. L. De Grosso, and A. Fuenzalida. Phlebotominae of epidemiological importance in cutaneous leishmaniasis in northwestern Argentina: risk maps and ecological niche models. Med. Vet. Entomol. 27:39–48. 2013.

50. R Development Core Team. R: a language and environment for statistical computing. 3.0.1 ed. R Foundation for Statistical Computing, Vienna, Austria. 2014.

51. Schoene, C. U., C. Staubach, C. Grund, A. Globig, M. Kramer, H. Wilking, M. Beer, F. J. Conraths, T. C. Harder, and B. L. M. Group. Towards a new, ecologically targeted approach to monitoring wild bird populations for avian influenza viruses. Epidemiol. Infect. 141:1050–1060. 2013.

52. Scholte, R. G., O. S. Carvalho, J. B. Malone, J. Utzinger, and P. Vounatsou. Spatial distribution of Biomphalaria spp., the intermediate host snails of Schistosoma mansoni, in Brazil. Geospat. Health 6:S95–S101. 2012.

53. Slater, H., and E. Michael. Predicting the current and future potential distributions of lymphatic filariasis in Africa using maximum entropy ecological niche modelling. PLoS One 7:e32202. 2012.

54. Soberón, J. Interpretation of models of fundamental ecological niches and species' distributional areas. University of Kansas, Lawrence. 2005.

55. Wallace, R. G., and W. M. Fitch. Influenza A H5N1 immigration is filtered out at some international borders. PLoS One 3:e1697. 2008.

56. Wetland International, Ramsar sites database. [2007; accessed 2016 Jan 21]. Available from: http://www.wetlands.org

57. Willeberg, P., A. Perez, M. Thurmond, M. Ascher, T. Carpenter, and M. AlKhamis. Visualization and analysis of the Danish 2006 highly pathogenic avian influenza virus H5N1 wild bird surveillance data by a prototype avian influenza BioPortal. Avian Dis. 54:433–439. 2010.

58. Williams, R. A., F. O. Fasina, and A. T. Peterson. Predictable ecology and geography of avian influenza (H5N1) transmission in Nigeria and West Africa. Trans. R. Soc. Trop. Med. Hyg. 102:471–479. 2008.

59. Williams, R. A., and A. T. Peterson. Ecology and geography of avian influenza (HPAI H5N1) transmission in the Middle East and northeastern Africa. Int. J. Health Geogr. 8:47. 2009.

60. Xu, X., Subbarao, N. J. Cox, and Y. Guo. Genetic characterization of the pathogenic influenza A/Goose/Guangdong/1/96 (H5N1) virus: similarity of its hemagglutinin gene to those of H5N1 viruses from the 1997 outbreaks in Hong Kong. Virology 261:15–19. 1999.

ACKNOWLEDGMENT

We are grateful to Preben Willeberg for assistance with revising this manuscript.